

Unraveling the Crystallization Kinetics of Supercooled Liquid GeTe by Ultrafast Calorimetry

Yimin Chen,^{†,‡,§} Guoxiang Wang,[‡] Lijian Song,^{†,§} Xiang Shen,^{*,‡} Junqiang Wang,^{*,†} Juntao Huo,[†] Rongping Wang,[‡] Tiefeng Xu,^{†,‡} Shixun Dai,[‡] and Qihua Nie[‡]

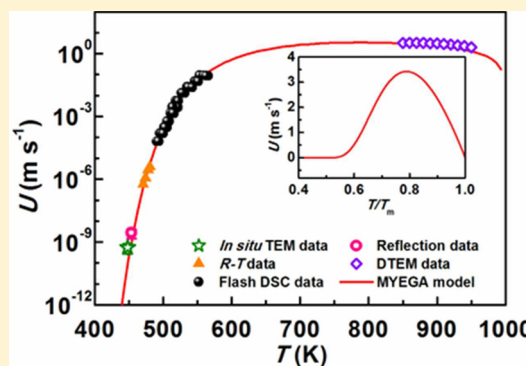
[†]Key Laboratory of Magnetic Materials and Devices & Zhejiang Province Key Laboratory of Magnetic Materials and Application Technology, Ningbo Institute of Materials Technology & Engineering, Chinese of Sciences, Ningbo, 315201, China

[‡]Laboratory of Infrared Material and Devices & Key Laboratory of Photoelectric Materials and Devices of Zhejiang Province, Advanced Technology Research Institute, Ningbo, 315211, China

[§]University of Chinese Academy of Sciences, Beijing, 100049, China

Supporting Information

ABSTRACT: Crystallization kinetics of phase change materials (PCMs) at high temperatures is of key importance for the extreme speed of data writing and erasing. In this work, the crystallization behavior of one of the typical PCMs, GeTe, has been studied using ultrafast differential scanning calorimetry (DSC) at high heating rates up to $4 \times 10^4 \text{ K s}^{-1}$. A strong non-Arrhenius temperature-dependent viscosity has been observed. We considered two viscosity models for estimating the crystal growth kinetics coefficient (U_{kin}). The results showed that the MYEGA model was more suitable to describe the temperature-dependent viscosity and the crystal growth kinetics for supercooled liquid GeTe. The glass transition temperature (T_g) and fragility m were estimated to be 432.1 K and 130.7, respectively. The temperature-dependent crystal growth rates, which were extrapolated by the MYEGA model, were in line with the experimental results that were measured by in situ transmission electron microscopy at a given temperature. The crystal growth rate reached a maximum of 3.5 m s^{-1} at 790 K. These results based on ultrafast DSC with the MYEGA model offer a revelation for crystallization kinetics of supercooled liquid GeTe.



1. INTRODUCTION

Phase change materials (PCMs), which switch reversibly between amorphous and crystalline phases to offer a large optical or electrical contrast, have been demonstrated to be promising for the next generation memory technology.^{1–3} Phase change kinetics, especially crystallization kinetics, which is of vital importance for the applications, has been widely investigated in experiments^{4–6} and molecular dynamics simulations.^{7–9} Differential scanning calorimetry (DSC) has been demonstrated to be a useful method for studying the crystallization kinetics of PCMs. However, in the past few decades, due to a low heating rate ($0.01\text{--}2 \text{ K s}^{-1}$) of conventional DSC, the investigation of the crystallization kinetics has been limited to a narrow temperature range near the glass transition temperature (T_g). This is much lower than the real application temperature of PCMs where the crystallization always happens at higher temperatures when it is heated by optical or electrical pulses at ultrafast heating rates.

Recently, ultrafast differential scanning calorimetry (ultrafast DSC) has been developed with the capability of a heating or cooling rate up to $1 \times 10^6 \text{ K s}^{-1}$.¹⁰ Such a high heating rate makes it possible to extend the crystallization kinetics analysis to a wider temperature range that is approaching its maximum

for some liquids. In 2012, Orava et al. first applied ultrafast DSC to study the conventional PCM $\text{Ge}_2\text{Sb}_2\text{Te}_5$ (GST),¹¹ where the temperature dependence of viscosity for GST was unexpectedly found to exhibit strong non-Arrhenius kinetics. Moreover, a fragile-to-strong transition was confirmed on cooling the liquid of widely used rewritable optical disc materials known as PCM $\text{Ag-In-Sb}_2\text{Te}$ (AIST),¹² and this explained the discrepancy between switching speed and data retention. Another growth-dominated PCM Ge_7Sb_9 has been revealed,¹³ and its fragility was moderate but its crystal growth rate was ultrafast. All these demonstrate that the ultrafast DSC is powerful in studying the crystallization kinetics of PCMs.

However, the models for analyzing crystallization kinetics are different among three PCMs, e.g., GST, AIST, and Ge_7Sb_9 . Orava et al. used the Cohen and Grest (C&G) model for GST¹¹ and applied the generalized-MYEGA (g-MYEGA) model for AIST that was developed from the Mauro–Yue–Ellison–Gupta–Allan (MYEGA) equation.¹² The C&G and MYEGA models were applied for Ge_7Sb_9 .¹³ However, the

Received: February 21, 2017

Revised: May 9, 2017

Published: May 19, 2017

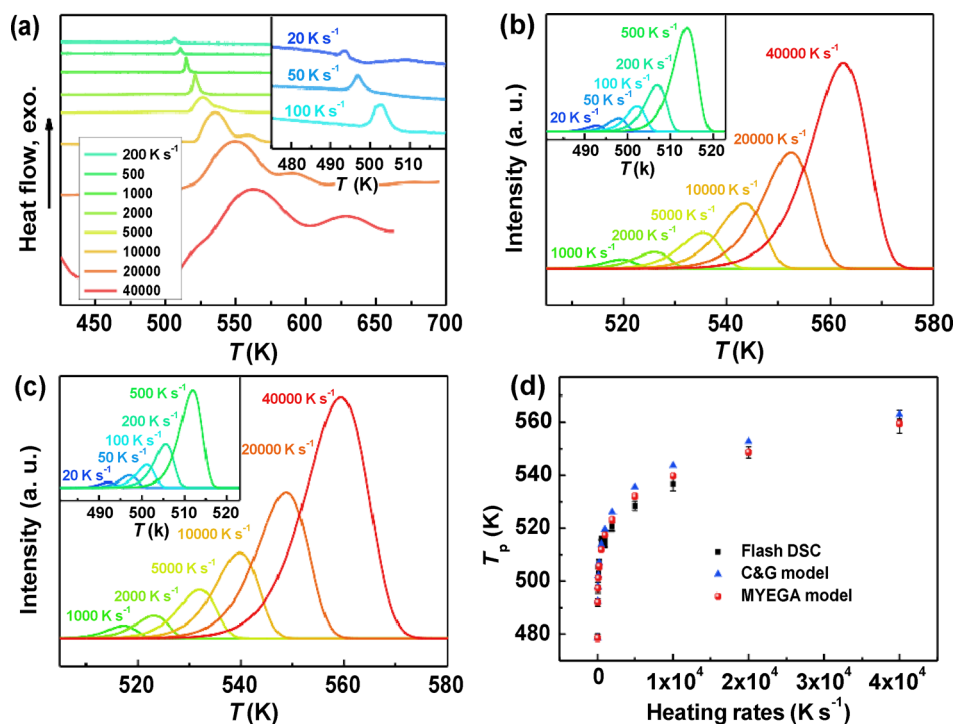


Figure 1. (a) Flash DSC traces of amorphous GeTe at heating rates from 20 to 40000 K s^{-1} . JMA numerical simulated DSC traces for GeTe by (b) C&G model and (c) MYEGA model, respectively. (d) The T_p values of ultrafast DSC tests and JMA numerical simulations. The black squares with error bar are Flash DSC data, the blue triangles are simulated results with C&G model, and the red spheres are simulated results with MYEGA model.

predicted crystal growth rate was not verified by experimental results in the work of GST materials.¹¹ Chen et al. evaluated crystal growth rates via detecting the crystal size at different temperatures to confirm that the MYEGA model was more suitable than the C&G model for the kinetics study.¹³ Although some of the crystallization temperatures came from the estimation via the laser power with assuming Arrhenius-type growth behavior, rather than being measured directly in Ge–Sb alloy,¹⁴ it might be the first time to confirm the calorimetric and extrapolated data by detecting crystal growth rates. Nevertheless, complete results of the crystallization temperature via experimental measurement are highly desired in both Ge–Sb and other systems.

Compared with GST, the GeTe alloy is of interest for PCM applications at high temperatures due to its higher crystallization temperature and larger activation energy.¹⁵ Given the simple atomic composition, GeTe is also a good model for studying the phase change kinetics. Recently, molecular dynamics simulations have been applied to analyze kinetics of the supercooled liquid state of GeTe at ultrafast heating rates,^{10,16–18} and some physical parameters such as the viscosity, diffusivity, fragility, and crystal growth rate have been achieved. It has been confirmed that the fast crystallization in GeTe is due to the large atomic mobility above T_g , but such simulation results have not been verified by experiments yet.

In this work, we have studied the crystallization kinetics of supercooled liquid GeTe by the ultrafast DSC. Two viscosity models, e.g., C&G and MYEGA, were applied to analyze the experimental results. The results demonstrated that MYEGA model was more suitable to describe the temperature-dependent viscosity and crystallization kinetics for supercooled liquid GeTe compared to the C&G model. We employed in situ transmission electron microscopy (TEM) to explore the

real crystal growth rate at a heating rate of 10 K min^{-1} , and the result was in agreement with the crystal growth rate of supercooled liquid GeTe that was extrapolated from the ultrafast DSC test.

2. EXPERIMENTAL METHODS

Amorphous GeTe films were deposited on $\text{SiO}_2/\text{Si}(100)$ by the magnetron sputtering method using a stoichiometric GeTe target. In each deposition, the base and working pressures were set to 2.5×10^{-4} Pa and 0.35 Pa, respectively. The thickness of the film was $1.4 \mu\text{m}$ that was in situ controlled by a thickness monitor equipped in the chamber and further checked by a Veeco Dektak 150 surface profiler. Another thinner film with a thickness of 25 nm was deposited on copper meshes with holey carbon films for in situ transmission electron microscopy (TEM) observation. The composition of the film was examined by energy dispersive spectroscopy (EDS). The sheet resistances of the as-deposited films as a function of elevated temperature (R – T) were in situ measured using the four-probe method in a homemade vacuum chamber.

The Mettler-Toledo Flash DSC 1, operated on the principles described by Zhuravlev and Schick,¹⁹ was employed to investigate the crystallization kinetics for PCMs. GeTe samples were scratched off from the glass substrates and loaded on the chip sensors. Then these samples were heated at the rates from 20 to 40000 K s^{-1} in an argon-protected atmosphere. For accuracy, the measurements were repeated more than four times at each heating rate. We used the Biot number, which was employed by Orava et al.,¹¹ to evaluate the potential thermal lag at the testing process. The Biot number is defined as $Bi = hL/\kappa$, where h is the heat-transfer coefficient between the heater and surface (a typical value is from 2 to 20 $\text{kW m}^{-2} \text{K}^{-1}$, which is also reasonable in this work and has been confirmed in the Supporting Information), L is the sample thickness (1400 nm in here) and κ is the thermal conductivity of the sample ($0.5 \text{ W m}^{-1} \text{K}^{-1}$ for amorphous GeTe at 300 K).²⁰ Taking these values, the Bi is in a range of 0.0056–0.056, which is much lower than the 0.1, indicating the thermal lag between sample and heater surface can be negligible.¹¹

Numerical simulations of DSC peaks were performed in this work. The heating was approximated as a series of isothermal steps with a step of 0.05 K. The crystallized volume fraction was calculated by successive application of Johnson–Mehl–Avrami (JMA) kinetics.^{21–24} The details are shown in the Supporting Information. Finally, the transformed volume was calculated at each temperature.

The TEM (JEOL 2100F) with an in situ heating holder (Gatan 628) was employed to observe the whole crystal growth process,²⁵ and the heating rate is 10 K min⁻¹. To eliminate the undesirable electron-induced crystallization in GeTe film, the observing area was extended to ~5 μm² to decrease the power density of the electron beam operated at 200 kV.

3. RESULTS AND DISCUSSION

3.1. Ultrafast Calorimetry Tests and Numerical Simulations. Figure 1a displays the typical ultrafast DSC heating flow traces for GeTe at various heating rates. The obvious exothermic peaks confirm an amorphous to crystal transformation during heating. The crystallization temperature (T_p), which corresponds to the position of the exothermic peak, as shown in Figure 1a, increases from 493 to 560 K when the heating rate increases from 20 to 40000 K s⁻¹. To unravel the contribution from nucleation and growth, a simplified description of nucleation and JMA kinetics theory was used to determine the growth rate of GeTe following that in ref 26 (see Supporting Information for details). Figure 1b,c shows the DSC traces from JMA numerical simulation for two models, i.e., C&G and MYEGA, respectively. Figure 1d depicts the T_p values of ultrafast DSC tests and JMA numerical simulations. It is evident that the simulated T_p values from both models are consistent with the experimental data.

3.2. Kissinger Analysis. The Kissinger equation for crystallization can be expressed as²⁶

$$\ln(\phi/T_p^2) = -Q/RT_p + A \quad (1)$$

where ϕ is the heating rate, T_p is the crystallization temperature, Q is the activation energy for crystallization, R is the gas constant, and A is a constant, respectively. At low heating rates, the value of Q is a constant, and then the relationship between $\ln(\phi/T_p^2)$ and $1/T_p$ is linear. So, the Kissinger plot of conventional DSC results usually yields an Arrhenius behavior. As shown in Figure 2, the $R-T$ data exhibit a linear Arrhenius behavior with $Q = 357$ kJ mol⁻¹ (see details in Supporting Information), while the activation energy Q decreases toward higher temperatures as expected for a fragile liquid since the ultrafast DSC data are curved.

3.3. Crystal Growth Kinetics. As Orava et al. suggested that the signal of DSC is related to crystal growth rate U , but not directly to the kinetics coefficient U_{kin} .²⁶ Therefore, the crystal growth rate U is given as²⁷

$$U = U_{kin}[1 - \exp(-\Delta G/RT)] \quad (2)$$

with R the gas constant and ΔG the driving force for crystallization. For ΔG , here, we used the equation of Thompson and Spaepen,²⁸ which is applicable for fragile chalcogenide liquids.²⁹ The equation can be written as

$$\Delta G = \frac{\Delta H_m \Delta T}{T_m} \left(\frac{2T}{T_m + T} \right) \quad (3)$$

where $\Delta H_m = 17.9$ kJ mol⁻¹ is latent heat of melting,¹⁶ $T_m = 1000$ K is the melting temperature,³⁰ and $\Delta T = T_m - T$ is the undercooling temperature.

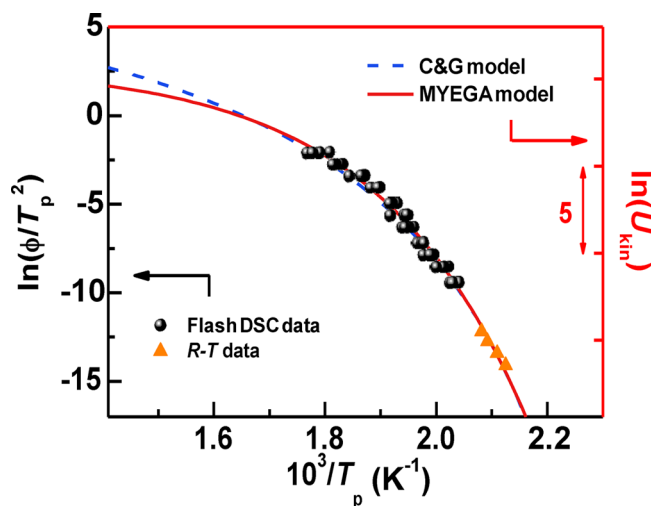


Figure 2. Kissinger plot for crystallization of supercooled liquid GeTe and the crystallization kinetics fitting by two models. Black circles are the experimental data from ultrafast DSC (the heating rate from 20 to 40000 K s⁻¹). For each heating rate, T_p slightly change due to the experimental errors, while the value of $\ln(\phi/T_p^2)$ is almost constant. The orange triangles are the T_p values from $R-T$ test in the same GeTe film (the heating rate from 10 to 70 K min⁻¹). The blue dashed curve is fitted by the C&G model, and the red curve is fitted by MYEGA model.

According to classical nucleation theory,³¹ crystal growth rate is given as $U \propto D [1 - \exp(-\Delta G/k_B T)]$. Thus, the kinetic coefficient for crystal growth U_{kin} is proportional to the diffusivity D , $U_{kin} \propto D$. Since a Stokes–Einstein relation between D and viscosity η is $D \propto 1/\eta$,³² a relationship can be obtained as $U_{kin} \propto D \propto 1/\eta$. Here, the C&G and MYEGA models are taken into account for the temperature-dependent viscosity (see Supporting Information for details). We got two U_{kin} expressions,

$$\log_{10} U_{kin} = A - \left(\frac{2B}{T - T_0 + [(T - T_0)^2 + 4CT]^{1/2}} \right) \quad (4)$$

and

$$\log_{10} U_{kin} = C_1 - \log_{10} \eta_\infty - (12 - \log_{10} \eta_\infty) \frac{T_g}{T} \exp \left[\left(\frac{m}{12 - \log_{10} \eta_\infty} - 1 \right) \left(\frac{T_g}{T} - 1 \right) \right] \quad (5)$$

from C&G and MYEGA models, respectively. These expressions are used to fit the T_p values to describe the temperature dependence of U_{kin} , which are shown in Figure 2. For the C&G model, the given parameters are $A = 3.56 \pm 0.023$, $B = 374.8 \pm 1.36$ K, $C = 1.7 \pm 0.01$, and $T_0 = 393.5 \pm 0.41$ K, respectively, with the quality of the fit as $R^2 = 0.9758$. According to the estimation of ref 17., the T_g of GeTe should be more than 400 K, which is higher than the parameter T_0 . However, Cohen and Grest found that T_0 would be 10–17% higher than T_g in their materials.³³ For the MYEGA model, the given parameters are $C_1 = -2.0 \pm 0.02$, $\log_{10} \eta_\infty = -3.2 \pm 0.05$, $T_g = 432.1 \pm 0.56$ K, and $m = 130.7 \pm 0.30$, respectively, with the quality of the fit as $R^2 = 0.9776$. The fittings satisfy the $R-T$ data and ultrafast DSC data, as shown in Figure 2.

3.4. Viscosity and Fragility. The temperature dependence of viscosity in the supercooled liquid can vary significantly between different materials. Angell proposed to use fragility m to describe the degree of deviation of viscosity η from an Arrhenius behavior,³⁴

$$m = [\partial \log_{10} \eta / \partial (T/T_g)]_{T=T_g} \quad (6)$$

As we know, once the temperature is above T_g , the viscosity of a “strong” liquid exhibits a weak temperature dependence in Arrhenius behavior, while for the viscosity of a “fragile” liquid decreases much faster along with increasing temperature in a non-Arrhenius way.³⁵ The high fragility indicates a relative fast crystallization speed in a large temperature range at relatively high temperatures.

Figure 3 shows Angell plots for temperature-dependent viscosity η for GeTe calculated by two models. It is worthy to

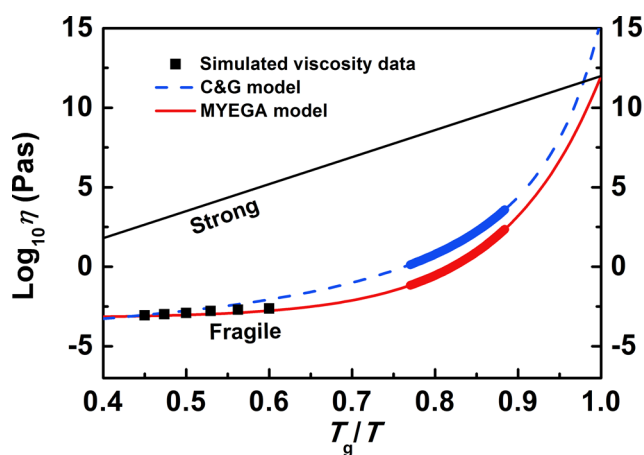


Figure 3. Angell plots for temperature dependence of viscosity. The blue dashed curve represents the fitting by the C&G model, in which the viscosity at T_m is fixed to $10^{-3.05}$ Pa s.¹⁶ The red solid curve represents the fitting by the MYEGA model. The thick regions in above two curves represent the temperature region of ultrafast DSC data. The black squares are simulated viscosity data from ref 16.

point out that C&G model does not contain required T_g and thus T_g of 432.1 K is used in Figure 3 for the C&G model that is estimated from the MYEGA model. For the C&G fitting, the viscosity at T_m is fixed to $10^{-3.05}$ Pa s.¹⁸ Nevertheless, the viscosity at T_g of $\sim 10^{15}$ Pa s is larger than that of the standard value (10^{12} Pa s), indicating that the fitting result at low temperature (around T_g) by the C&G model is overestimated. Moreover, the fragility m , which can be obtained by eq 6, is 207. This value is larger than that of the typical fragile liquid PVC ($m \approx 191$).³⁷ Therefore, although the C&G model may be suitable for the crystallization kinetics and viscosity analysis of GST supercooled liquid, it might not be suitable to explain that of GeTe liquid.

We achieved the viscosity at infinite temperature, fragility, and T_g from MYEGA fitting. The viscosity at the infinite temperature of GeTe is consistent with that suggested by Mauro et al.³⁶ As shown in Figure 3, the viscosity at T_m is also close to $10^{-3.05}$ Pa s that is estimated by dynamic molecular simulation.¹⁷ The fragility of the supercooled liquid GeTe we achieved is larger than that of GST.¹¹ For the T_g of PCMs, direct results are not available due to the experimental difficulty. According to Kalb et al.,³⁸ T_g is related to the crystallization temperature T_p in PCMs, it is about 10 K below T_p at a heating

rate of 40 K min^{-1} . However, it was found that the T_g estimated from the MYEGA model is about 40–60 K lower than T_p .¹⁴ Here we determined T_p to be ~ 478 K using R–T test at a heating rate of 40 K min^{-1} . Thus, T_g ($= 432.1$ K) determined here by the MYEGA model is reasonable. Therefore, the fitting by the MYEGA model yields more reasonable results to unravel the crystallization kinetics and liquid’s viscosity compared to the C&G model.

3.5. Crystal Growth Rates. The MYEGA viscosity model does give a good fit for the crystallization kinetics coefficient and viscosity, and thus is a good model for extrapolating the crystal growth rates to higher temperatures. By employing eq 2, eq 3, and eq 5, with the parameters in section 3.3, the crystal growth rate is estimated by the MYEGA model at a temperature range from T_g to T_m . As shown in Figure 4, the

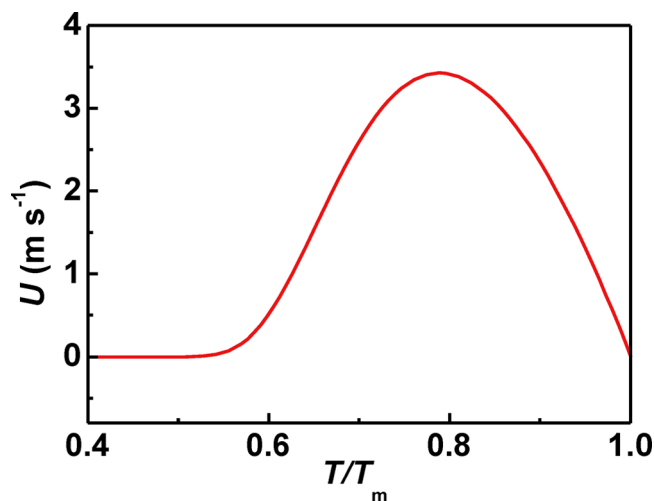


Figure 4. Temperature-dependent crystal growth rates for supercooled liquid GeTe that is extrapolated by the MYEGA model.

crystal growth rate reaches the maximum, $U_{\max} = 3.5 \text{ m s}^{-1}$ at $0.79 T_m$. This U_{\max} is similar to that of GST, AIST, and other PCMs.^{11,12,16,39,40,41} The estimated T_g is 432.1 K, and the T_{\max} is 790 K; thus T_{\max} is 1.8 times of T_g , which is slightly larger than that was concluded in ref 42; i.e., $T_{\max} = 1.48 \pm 0.15 T_g$.

The in situ TEM images for GeTe film at a heating rate of 10 K min^{-1} are shown in Figure 5. The corresponding in situ TEM video is shown in Supporting Information. Figure 5a shows the TEM image at the temperature is 423 K. Clearly, the film is still in the amorphous state. There are some nanosized grains in the film when the temperature increases to 433 K as shown in Figure 5b, which implies the crystal grains begin to grow at this temperature. The crystal grains grow rapidly with increasing temperature from 443 to 463 K as shown in Figure 5c–e, and the growth ends at a temperature of 463 K because of no significant change of grain size with further increasing temperature up to 473 K in Figure 5f. We determined the value of T_p , that is the temperature with the fastest crystal growth rate, to be 448 K from the in situ TEM video (see Supporting Information). This is in line with the result that was reported in ref 43. Moreover, there is almost no formation of the new grains when the temperature is above T_p , indicating that the number density of the nucleation centers N is most likely saturated upon heating. So it is reasonable to consider N as a constant used in the JMA numerical simulation. This saturated N can be estimated by the crystal numbers under the

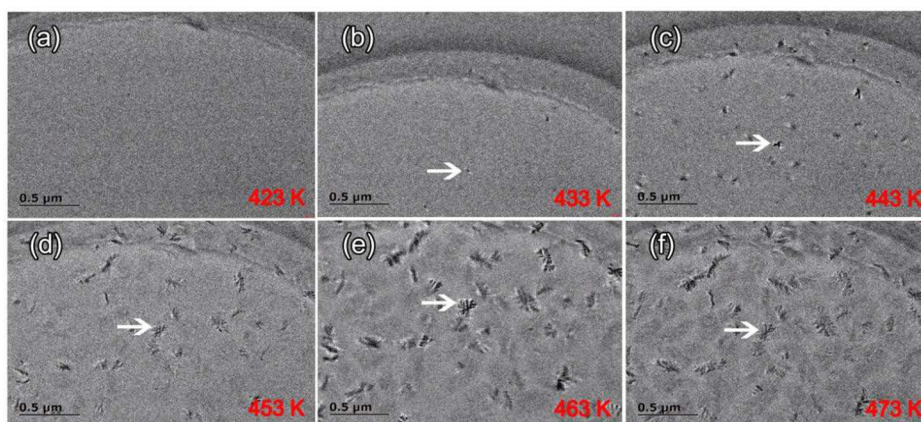


Figure 5. In situ TEM images of GeTe film at a continuous heating rate of 10 K min^{-1} : (a) 423 K, (b) 433 K, (c) 443 K, (d) 453 K, (e) 463 K, and (f) 473 K. The arrows in the figures are used to trace the growth of specific crystal grain. The onset and end temperatures of crystal growth are estimated to be 433 and 463 K, between which the density of crystals is almost constant. The value of T_p that is the temperature with the fastest crystal growth rate is determined as 448 K.

view field of TEM. The details of this estimation are shown in Supporting Information. We used N of $1 \times 10^{15} \text{ mol}^{-1}$ in the numerical simulation for this work.

Figure 6 shows the crystal growth rate that is extrapolated from the MYEGA model (red line) for GeTe in the temperature

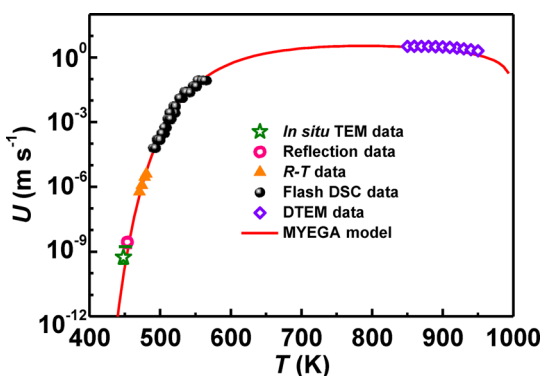


Figure 6. Crystal growth rate for GeTe in temperature range from T_g to T_m . The green star is the crystal growth rate measured by in situ TEM. The orange triangles and black circles are evaluated by $R-T$ data and flash DSC data, respectively. The purple diamonds are measured by DTEM.⁴⁰ The pink circle is the crystal growth rate estimated by optical reflection data.⁴³ The red curve is the fitting result according to the MYEGA model.

range from T_g to T_m . Recently, the crystal growth rate near to T_m was evaluated by a method named dynamic TEM (DTEM).⁴⁰ As shown in Figure 6, we can see the DTEM result (purple diamonds) is in line with that of extrapolated by the MYEGA model at the high temperature range. To further verify the reliability of the MYEGA model, the crystal growth rates (U) are estimated experimentally by measuring the crystal size (d) and the crystallization time (t) with the expression:⁴⁴

$$U = d/2t \quad (7)$$

As shown in Figure 5e,f, the grains with different shapes are due to the anisotropy of the crystal growth. The arrow in the Figure 5 is used to trace the growth for a specific crystal grain. We evaluated all of the crystal size in the field of view as shown in Figure 5e, and it shows the value of d is in the range of 100–300 nm. For the corresponding crystallization time t , it is ~ 3

min, which can be roughly calculated by the heating rate and the onset/end temperature of crystal growth in Figure 5. Therefore, the crystal growth rate at specific temperature of 448 K (the estimated T_p value) can be estimated by eq 7 as $5.6 \pm 2.8 \times 10^{-10} \text{ m s}^{-1}$. In addition, from the optical reflection data that was reported by Libera et al.,⁴³ the crystal growth rate can be estimated as $2.8 \pm 1.3 \times 10^{-9} \text{ m s}^{-1}$ at a temperature of 453.6 K. They are shown as symbols in Figure 6. Together with the extrapolated $R-T$ and flash DSC results (orange triangles and black circles in Figure 6), all these are also in good agreement with the theoretical rate that is extrapolated by the MYEGA model. Therefore, the extrapolated temperature dependence of the crystal growth rate is in accordance with both the high and low temperature range, which demonstrates the MYEGA model employed here to analyze the ultrafast DSC data is reliable. It also suggests that the ultrafast DSC is a significant method to investigate the crystallization kinetics of the supercooled liquid PCM alloy.

4. CONCLUSIONS

The crystallization of GeTe amorphous films has been studied at heating rates from 20 to 40000 K s^{-1} by ultrafast DSC. Using the MYEGA model, the viscosity at infinite temperature η_∞ , the glass transition temperature T_g , and fragility m are determined to be $10^{-3.2} \text{ Pa s}$, 432.1 K, and 130.7, respectively. The temperature-dependent crystal growth rates are obtained with the U_{\max} of 3.5 m s^{-1} at a temperature of 790 K ($0.79 T_m$) for GeTe. Crystal growth rate estimated by in situ TEM is in line with the result from the MYEGA model extrapolation. It further confirms that the MYEGA model is reliable for unraveling the crystallization kinetics of supercooled liquid GeTe. The large fragility and high activation energy for crystallization at the low temperature range account for a fast phase transition speed and good thermal stability. It indicates GeTe is a promising phase change material for long-data retention at high temperatures.

■ ASSOCIATED CONTENT

Supporting Information

The Supporting Information is available free of charge on the ACS Publications website at DOI: 10.1021/acs.cgd.7b00259.

Figures and formulas showing the detailed numerical simulation by the JMA kinetics theory, the estimation of crystallization temperature and activation energy for crystallization of GeTe by the $R-T$ method, and two viscosity methods and the corresponding transferred U_{kin} expressions (PDF)

A video showing the crystal growth process at a low heating rate of 10 K min^{-1} by in situ TEM (AVI)

AUTHOR INFORMATION

Corresponding Authors

*(X.S.) E-mail: shenxiang@nbu.edu.cn.

*(J.W.) E-mail: jqwang@nimte.ac.cn.

ORCID

Yimin Chen: [0000-0002-3057-5062](https://orcid.org/0000-0002-3057-5062)

Notes

The authors declare no competing financial interest.

ACKNOWLEDGMENTS

This work was financially supported by the Natural Science Foundation of China (Grant Nos. 61377061, 61604083, 11504931), the Public Project of Zhejiang Province (Grant No. 2014C31146), the Natural Science Foundation of Zhejiang Province (Grant No. LQ15F040002), One Hundred Talents Program of Chinese Academy of Sciences. Authors are grateful to Prof. F. Rao and Dr. K. Ding for the in situ TEM measurements.

REFERENCES

- (1) Ovshinsky, S. R. Reversible electrical switching phenomena in disordered structures. *Phys. Rev. Lett.* **1968**, *21* (20), 1450–1453.
- (2) Wuttig, M.; Yamada, N. Phase-change materials for rewriteable data storage. *Nat. Mater.* **2007**, *6* (11), 824–832.
- (3) Wuttig, M. Phase-change materials: towards a universal memory? *Nat. Mater.* **2005**, *4* (4), 265–266.
- (4) Park, J.; Kim, M. R.; Choi, W. S.; Seo, H.; Yeon, C. Characterization of amorphous phases of $\text{Ge}_2\text{Sb}_2\text{Te}_5$ phase-change optical recording material on their crystallization behavior. *Jpn. J. Appl. Phys.* **1999**, *38* (8R), 4775.
- (5) Kalb, J.; Spaepen, F.; Wuttig, M. Atomic force microscopy measurements of crystal nucleation and growth rates in thin films of amorphous Te alloys. *Appl. Phys. Lett.* **2004**, *84* (25), 5240–5242.
- (6) Raoux, S.; Ielmini, D.; Welnic, W. Phase change materials and their application to nonvolatile memories. *Chem. Rev.* **2010**, *110* (1), 240–267.
- (7) Hegedüs, J.; Elliott, S. Microscopic origin of the fast crystallization ability of Ge–Sb–Te phase-change memory materials. *Nat. Mater.* **2008**, *7* (5), 399–405.
- (8) Matsunaga, T.; Akola, J.; Kohara, S.; Honma, T.; Kobayashi, K.; Ikenaga, E.; Jones, R. O.; Yamada, N.; Takata, M.; Kojima, R. From local structure to nanosecond recrystallization dynamics in AgInSbTe phase-change materials. *Nat. Mater.* **2011**, *10* (2), 129–134.
- (9) Sosso, G. C.; Colombo, J.; Behler, J. r.; Del Gado, E.; Bernasconi, M. Dynamical heterogeneity in the supercooled liquid state of the phase change material GeTe. *J. Phys. Chem. B* **2014**, *118* (47), 13621–13628.
- (10) Zhuravlev, E.; Madhavi, V.; Lustiger, A.; Androsch, R.; Schick, C. Crystallization of polyethylene at large undercooling. *ACS Macro Lett.* **2016**, *5* (3), 365–370.
- (11) Orava, J.; Greer, A.; Gholipour, B.; Hewak, D.; Smith, C. Characterization of supercooled liquid $\text{Ge}_2\text{Sb}_2\text{Te}_5$ and its crystallization by ultrafast-heating calorimetry. *Nat. Mater.* **2012**, *11* (4), 279–283.

(12) Orava, J.; Hewak, D. W.; Greer, A. L. Fragile-to-strong crossover in supercooled liquid Ag–In–Sb–Te studied by ultrafast calorimetry. *Adv. Funct. Mater.* **2015**, *25* (30), 4851–4858.

(13) Chen, B.; Momand, J.; Vermeulen, P. A.; Kooi, B. J. Crystallization kinetics of supercooled liquid Ge–Sb based on ultrafast calorimetry. *Cryst. Growth Des.* **2016**, *16* (1), 242–248.

(14) Eising, G.; Van Damme, T.; Kooi, B. J. Unraveling crystal growth in GeSb phase-change films in between the glass-transition and melting temperatures. *Cryst. Growth Des.* **2014**, *14* (7), 3392–3397.

(15) Ghezzi, G.; Raty, J.-Y.; Maitrejean, S.; Roule, A.; Elkaim, E.; Hippert, F. Effect of carbon doping on the structure of amorphous GeTe phase change material. *Appl. Phys. Lett.* **2011**, *99* (15), 151906.

(16) Sosso, G. C.; Miceli, G.; Caravati, S.; Giberti, F.; Behler, J. r.; Bernasconi, M. Fast crystallization of the phase change compound GeTe by large-scale molecular dynamics simulations. *J. Phys. Chem. Lett.* **2013**, *4* (24), 4241–4246.

(17) Sosso, G. C.; Behler, J.; Bernasconi, M. Breakdown of Stokes–Einstein relation in the supercooled liquid state of phase change materials. *Phys. Status Solidi B* **2012**, *249* (10), 1880–1885.

(18) Sosso, G. C.; Salvalaglio, M.; Behler, J. r.; Bernasconi, M.; Parrinello, M. Heterogeneous crystallization of the phase change material GeTe via atomistic simulations. *J. Phys. Chem. C* **2015**, *119* (11), 6428–6434.

(19) Zhuravlev, E.; Schick, C. Fast scanning power compensated differential scanning nano-calorimeter: 1. The device. *Thermochim. Acta* **2010**, *505* (1), 1–13.

(20) Nath, P.; Chopra, K. L. Thermal conductivity of amorphous and crystalline Ge and GeTe films. *Phys. Rev. B* **1974**, *10* (8), 3412–3418.

(21) Johnson, W. A.; Mehl, R. F. Reaction kinetics in processes of nucleation and growth. *Trans. AIME* **1939**, *135* (8), 396–415.

(22) Avrami, M. Kinetics of phase change. I General theory. *J. Chem. Phys.* **1939**, *7* (12), 1103–1112.

(23) Avrami, M. Kinetics of phase change. II transformation-time relations for random distribution of nuclei. *J. Chem. Phys.* **1940**, *8* (2), 212–224.

(24) Avrami, M. Granulation, phase change, and microstructure kinetics of phase change. III. *J. Chem. Phys.* **1941**, *9* (2), 177–184.

(25) Zheng, Y.; Xia, M.; Cheng, Y.; Rao, F.; Ding, K.; Liu, W.; Jia, Y.; Song, Z.; Feng, S. Direct observation of metastable face-centered cubic Sb_2Te_3 crystal. *Nano Res.* **2016**, *9* (11), 3453–3462.

(26) Orava, J.; Greer, A. Kissinger method applied to the crystallization of glass-forming liquids: Regimes revealed by ultrafast-heating calorimetry. *Thermochim. Acta* **2015**, *603*, 63–68.

(27) Ediger, M.; Harrowell, P.; Yu, L. Crystal growth kinetics exhibit a fragility-dependent decoupling from viscosity. *J. Chem. Phys.* **2008**, *128* (3), 034709.

(28) Thompson, C. V.; Spaepen, F. On the approximation of the free energy change on crystallization. *Acta Metall.* **1979**, *27* (12), 1855–1859.

(29) Battezzati, L.; Greer, A. Thermodynamics of $\text{Te}_{80}\text{Ge}_{20-x}\text{Pb}_x$ glass-forming alloys. *J. Mater. Res.* **1988**, *3* (03), 570–575.

(30) Hansen, M.; Anderko, K.; Salzberg, H. Constitution of binary alloys. *J. Electrochem. Soc.* **1958**, *105* (12), 260C–261C.

(31) Turnbull, D.; Fisher, J. C. Rate of nucleation in condensed systems. *J. Chem. Phys.* **1949**, *17* (1), 71–73.

(32) Einstein, A. *Investigations on the theory of non-uniform gases*. Dover Publisher: New York, 1956.

(33) Cohen, M. H.; Grest, G. Liquid-glass transition, a free-volume approach. *Phys. Rev. B: Condens. Matter Mater. Phys.* **1979**, *20* (3), 1077.

(34) Angell, C. A. Glass-formers and viscous liquid slowdown since David Turnbull: enduring puzzles and new twists. *MRS Bull.* **2008**, *33* (05), 544–555.

(35) Zhang, W.; Ronneberger, I.; Zalden, P.; Xu, M.; Salinga, M.; Wuttig, M.; Mazzarello, R. How fragility makes phase-change data storage robust: insights from ab initio simulations. *Sci. Rep.* **2015**, *4*, 6529.

- (36) Mauro, J. C.; Yue, Y.; Ellison, A. J.; Gupta, P. K.; Allan, D. C. Viscosity of glass-forming liquids. *Proc. Natl. Acad. Sci. U. S. A.* **2009**, *106* (47), 19780–19784.
- (37) Böhmer, R.; Ngai, K.; Angell, C. A.; Plazek, D. Nonexponential relaxations in strong and fragile glass formers. *J. Chem. Phys.* **1993**, *99* (5), 4201–4209.
- (38) Kalb, J.; Wuttig, M.; Spaepen, F. Calorimetric measurements of structural relaxation and glass transition temperatures in sputtered films of amorphous Te alloys used for phase change recording. *J. Mater. Res.* **2007**, *22* (03), 748–754.
- (39) Salinga, M.; Carria, E.; Kaldenbach, A.; Bornhofft, M.; Benke, J.; Mayer, J.; Wuttig, M. Measurement of crystal growth velocity in a melt-quenched phase-change material. *Nat. Commun.* **2013**, *4*, 2371.
- (40) Santala, M.; Reed, B.; Raoux, S.; Topuria, T.; LaGrange, T.; Campbell, G. Irreversible reactions studied with nanosecond transmission electron microscopy movies: Laser crystallization of phase change materials. *Appl. Phys. Lett.* **2013**, *102* (17), 174105.
- (41) Winseck, M.; Cheng, H.-Y.; Campbell, G.; Santala, M. Crystallization kinetics of the phase change material GeSb₂Te measured with dynamic transmission electron microscopy. *Dalton T.* **2016**, *45*, 9988–9995.
- (42) Orava, J.; Greer, A. Fast and slow crystal growth kinetics in glass-forming melts. *J. Chem. Phys.* **2014**, *140* (21), 214504.
- (43) Libera, M.; Chen, M. Time-resolved reflection and transmission studies of amorphous Ge-Te thin-film crystallization. *J. Appl. Phys.* **1993**, *73* (5), 2272–2282.
- (44) Wang, J.; Chen, N.; Liu, P.; Wang, Z.; Louzguine-Luzgin, D.; Chen, M.; Perepezko, J. The ultrastable kinetic behavior of an Au-based nanoglass. *Acta Mater.* **2014**, *79*, 30–36.